Int. J. Heat Mass Transfer. Vol. 15, pp. 327–339. Pergamon Press 1972. Printed in Great Britain

FREE CONVECTION HEAT TRANSFER FROM ISOTHERMAL SPHERES IN WATER

WAYNE S. AMATO and CHI TIEN

Department of Chemical Engineering and Metallurgy, Syracuse University, Syracuse, New York 13210, U.S.A.

(*Received* 22 *March* 1971)

Abstract—An experimental investigation of free convection heat transfer from heated spheres to water is reported. The experimental data extend over a wide range of Rayleigh number, thus covering the laminar, transition, and beginning of the turbulent regimes. The temperature and velocity fields around a heated isothermal sphere have been measured, with the velocity profiles determined from the use of hot-film anemometry techniques. When possible, the comparison of the experimental results with the prediction of theory shows good agreement.

NOMENCLATURE

c_p, specific heat per unit mass;
D, diameter;
f, function defined in equation (5);
g, acceleration due to gravity;
Gr, $g\beta\rho^2D^3\Delta T/\mu^2$ Grashof number;
$\overline{Nu}$, hD/k average Nusselt number;
Pr, $c_p\mu/k$ Prandtl number;
h, heat-transfer coefficient $= q/\Delta T$;
k, thermal conductivity;
q, heat flux;
R, radius of sphere or resistance;
r_1, r/R where r is the distance of a point on the surface from the axis of symmetry;
T, temperature;
T_w, wall temperature;
T_∞, bulk temperature;
u, velocity component in x-direction;
v, velocity component in y-direction;
x, distance along surface from stagnation point;
x_1, x/R dimensionless distance;
y, distance normal to the surface.

Greek letters

α, thermal diffusivity or temperature coefficient of resistance;
β, coefficient of thermal expansion;
ε, angle between the normal to the surface and the direction of the body force vector;
η, similarity variable;
ν, kinematic viscosity;
θ, dimensionless temperature $(T - T_\infty)/(T_w - T_\infty)$;
μ, viscosity;
ρ, density;
ϕ, angular position from stagnation point.

INTRODUCTION

THE FREE convective transport of thermal energy from a spherical surface in water is the concern of this paper. Heat transfer data from spheres in free convection has been obtained in air by Yuge [1] and Elenbaas [2]. Also, mass transfer data in the form of melting or dissolution experiments has yielded related free convection information [3–8]. Boberg and Starrett [9] have obtained some information on the heat transfer from a sphere to water. However, there does not appear to be any comprehensive, purely heat transfer study of free convection from spheres. This represents one objective of this study.

The second objective is concerned with the characterization to some extent of the temperature and velocity fields in free convective flow. The measurement of velocity fields in a liquid system can be accomplished by the tracking of small particles carried along by the flow [14], by the use of a quartz-film anemometer, or by hot-film anemometry. The problem is complicated in the case of hot-film anemometry by the fact that the temperature and velocity fields are coupled and, hence, a knowledge of their interrelationship is necessary. Nevertheless, it is possible to effectively utilize the hot-film anemometer in free-convective liquid systems. This work and the work of other investigators [15, 16] confirms this contention.

Theoretical characterization of free convection from a sphere has been carried out by Merk and Prins [17], Acrivos [18], and Chiang, Ossin and Tien [22]. The last mentioned is not applicable to our work since it is a numerical solution for the case of air with a Prandtl number of 0·70. The works of Merk and Prins [17] and Acrivos [18] will be utilized in the following section and will form the basis for the theoretical comparisons with our experimental work. Also, Saville [19], Saville and Churchill [20, 21] have treated the problem of free convection flow about two-dimensional and axisymmetric bodies of revolution.

THEORY

Acrivos [18] formulates the problem as follows: he seeks an asymptotic solution as as $Pr \to \infty$ in the region where inertia terms are unimportant, viz. inside the thermal boundary layer. The pertinent equations describing the system are (for axially symmetric flow):

$$u\frac{\partial u}{\partial x} + v\frac{\partial u}{\partial y} = g\beta(T_w - T_\infty)\,\theta \sin\varepsilon + \nu\frac{\partial^2 u}{\partial y^2} \tag{1}$$

$$\frac{\partial(ru)}{\partial x} + \frac{\partial(rv)}{\partial y} = 0 \tag{2}$$

$$u\frac{\partial\theta}{\partial x} + v\frac{\partial\theta}{\partial y} = \alpha\frac{\partial^2\theta}{\partial y^2} \tag{3}$$

subject to

$$\begin{aligned} &y = 0; \quad u = 0, \quad v = 0, \quad \theta = 1 \\ &y = \infty \quad \text{and} \quad x = 0. \quad u = 0, \quad \theta = 0. \end{aligned} \tag{4}$$

The asymptotic behavior of the above equations is investigated by allowing $Pr \to \infty$. A similarity transformation converts the equations to two simultaneous, ordinary differential equations. The similarity variables for the special case of a sphere are:

$$u = \frac{\sqrt{[gR\beta(T_w - T_\infty)]}}{Pr^{\frac{1}{2}}}(\sin x_1 \times \left[\frac{4}{3}\left(\frac{1}{\sin x_1}\right)^{\frac{8}{3}}\int_0^{x_1}(\sin x_1)^{\frac{5}{3}}\,dx_1\right]^{\frac{1}{2}} f'(\eta) \tag{5}$$

$$\theta = \theta(\eta) \tag{6}$$

where

$$\eta = \frac{\frac{y}{R}\left(\frac{Gr \cdot Pr}{8}\right)^{\frac{1}{4}}}{\left[\frac{4}{3}\left(\frac{1}{\sin x_1}\right)^{\frac{8}{3}}\int_0^{x_1}(\sin x_1)^{\frac{5}{3}}\,dx_1\right]^{\frac{1}{4}}}. \tag{7}$$

With the transformation, one arrives at

$$f''' + \theta = 0 \tag{8}$$

$$\theta'' + f\theta' = 0 \tag{9}$$

with the boundary conditions

$$\begin{aligned} &\theta(0) = 1, \quad \theta(\infty) = 0, \quad f(0) = 0 \\ &f'(0) = 0, \quad f''(\infty) = 0. \end{aligned} \tag{10}$$

Acrivos [18] has solved for $\theta'(0)$ and $f''(0)$ by a series expansion around $\eta = 0$. He obtains $-\theta'(0) = 0{\cdot}54$ and $f''(0) = 1{\cdot}08$. Equations (8) and (9) only apply in the region of the thermal boundary layer; thus, velocities obtained through the use of equations (5), (7), (8) and (9) would be confined to a narrow region where $f''(0) \geqslant 0$. With his values of $f''(0)$ and $\theta'(0)$, equations (8) and (9) can be readily integrated. The results are shown later.

The expression of the average Nusselt number for the sphere takes the form:

$$\overline{Nu} = 0{\cdot}583\,(Gr\,.\,Pr)^{\frac{1}{4}}. \qquad (11)$$

Merk and Prins' [17] work will be used to compare the values of maximum velocity measured in the velocity traverses. The results are in the form of a plot of $[u_{max}/(\nu/D)Gr^{\frac{1}{2}}]$ vs. the angular distance from the stagnation point, with Prandtl number as a parameter. Thus, it is quite easy to compare these values to the maximum obtained experimentally. Merk and Prins [17] obtain the following relationship between the Nusselt number and the Rayleigh number:

$$\overline{Nu} = 0{\cdot}558\,(Gr\,.\,Pr)^{\frac{1}{4}}. \qquad (12)$$

The basic theory for hot-wire anemometry was developed by King [23]. The "King's Law" relationship, although obtained through neglect of viscosity (i.e. using potential theory) represents a reasonable approximation in gases. However, in liquids, there are two additional complications: the conductance of the liquid which would short the wire and the large variation of physical properties with temperature. The first problem has been solved through the development of quartz-coated hot-film sensors. The second problem still exists and must be dealt with, usually most effectively by direct calibration. The characteristics of a sensor are determined by its temperature coefficient of resistance, which is defined by

$$R_H/R_C = 1 + \alpha_C(T_s - T_e) \qquad (13)$$

where the subscript, H, refers to the hot or operating resistance of the sensor, C refers to the environment, s refers to the sensor temperature and e refers to the environment. The ratio, R_H/R_C, is known as the "overheat ratio". For platinum films, α is usually 0·002–0·003/°C. In liquids, R_H/R_C usually does not exceed 1·1.

The proximity of the sensor to a surface can markedly influence the heat transfer from the sensor. Piercy, Richardson and Winney [24], Wills [25] and Richardson [26] have investigated this problem. It is more of a problem in gases than in liquids, since the heat transfer coefficient in gases is about two orders of magnitude lower. Estimations using the above works showed the problem to be small except at very close distances.

EXPERIMENTAL EQUIPMENT

Four sphere sizes were used in the experimental investigations, with nominal diameters of 1, 2, 3 and 4 in. The electrically heated spherical heat transfer elements were composed of the following parts: (a) copper hemispheres, (b) core, (c) nichrome winding, (d) support tube, and (e) thermocouples (see Fig. 1). See [27] for a more detailed description.

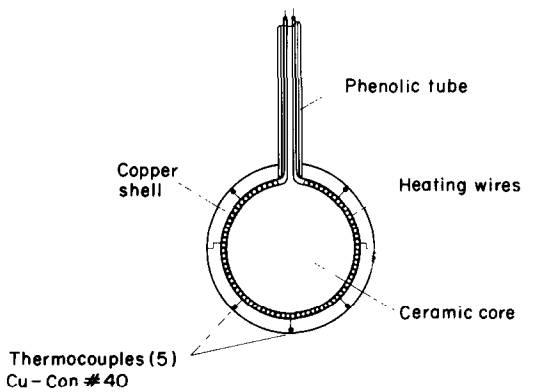

FIG. 1. Sphere construction.

The copper hemispheres enclosed the core on which the nichrome wire was wound. The copper wall was approximately $\frac{1}{8}$ in. thick. The two hemispheres fit snugly together by means of mating grooves in each hemisphere.

The core was formed by casting two separate hemispheres of Vel-Mix Stone precision molding compound in the respective copper hemisphere and then joining them together so as to form a perfectly fitting spherical core. Circular horizontal grooves were cut at a $\frac{1}{8}$ in. spacing on the surface of the core in order to allow for the nichrome winding. The core was then heated

for 24 hours at 150°C in order to drive off the water of hydration.

The winding was formed of either 24, 29 or 30 gauge nichrome wire depending on the resistance desired in order to achieve a certain power level. The wire was bonded to the core in the grooves and insulated using a rubber compound.

The support tube was used to suspend the sphere vertically in the water and also to feed the power leads and thermocouple wires into the sphere. The support tubes were made of a linen grade phenolic. Since there were microscopic pinholes in this material, the tubes were coated with six coats of spar varnish to insure waterproofing. The support tube was screwed into the upper copper hemisphere and sealed with an epoxy resin.

Five copper–constantan thermocouples of 40 B and S gauge wire were embedded in the copper walls inside the sphere. They were positioned in a vertical diametral plane, one at the stagnation point, two at the 45° positions, and two at the 135° positions. Calibrations were performed at two fixed points, viz. 50°C and 100°C according to procedures recommended in [28].

The mating surface of the two hemispheres was sealed with a thin layer of silicone rubber to prevent leakage of water into the sphere. The spheres were cleaned and polished before each set of runs so that a clean mirror-like surface was obtained.

All the heat transfer experiments were conducted in a rectangular, plexiglas tank 30 in. × 20 in. × 30 in. and of about 75 gallon capacity. The transparent nature of the tank was invaluable in the microscopic studies using the thermocouple and hot-film anemometer probes. The tank was mounted such that vibrations were minimized.

The power supply for the heating elements utilized 110 V a.c. which was regulated to 0·1 per cent by a voltage regulator and could be continuously varied using autotransformers. An additional transformer in the system enabled the effective voltage range to be extended to 280 V. Power to the spheres was measured by three precision wattmeters capable of $\frac{1}{4}$ per cent accuracy over a range of several watts to 1000 W. Provision was also made to accurately measure voltage and amperage.

The traversing mechanism enabled three-dimensional movement of the thermocouple and hot-film anemometer probes. This device was capable of accurate measurements to less than 0·001 in. It was constructed of three mutually orthogonal "Unislides". Scales were added so that readings in thousandths of an inch could be noted directly. The traversing mechanism was secured to a 3 in. thick by 2 ft long aluminium bed which was bolted to the top edge of the plexiglas tank, thereby yielding a stable configuration. Specific adapter rods were designed to best handle the particular probe in question.

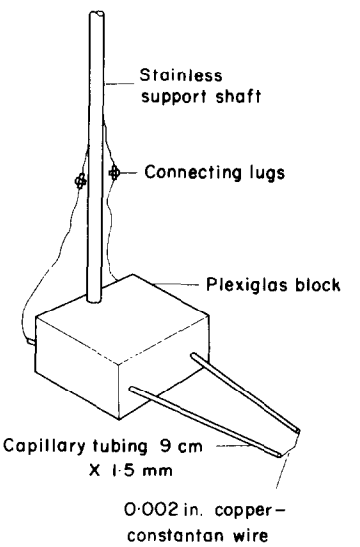

FIG. 2. Thermocouple probe construction.

The thermocouple probe was constructed of 0·002 in. copper–constantan wire. It is shown in Fig. 2. The probe was calibrated over a range of 20–60°C with six points using a difference curve calibration [28].

The hot-film anemometry equipment was

procured from Thermo-Systems, Inc., St. Paul, Minnesota. It is a constant-temperature hot-film anemometer and designated as a 1010A unit by Thermo-Systems, Inc. The probes used in this investigation were hot-film types, quartz-coated in order to be usable in a conducting fluid such as water. The probe used in the velocity measurement determinations was a 1212-10W, i.e. a probe with a 0·001 in. quartz-coated hot-film sensor.

Calibration of the probe over ranges of temperature and velocity was effected by means of two-tanks especially constructed for this purpose. Two were built: for horizontal and vertical tows. Essentially, they consisted of a probe-holder block which could run on rails by being dragged through the solution. The tanks had a traverse of about 15 in which is suitable for low velocity measurements. The power for towing was supplied by the chart drive of a recorder by means of a gearing arrangement designed for the purpose. The tanks were insulated and had a capacity of about 2 gallons.

A directional mounting device was constructed for use with a cantilever type hot-film probe. This type of probe registers a maximum when the flow is normal to the cylindrical element and a minimum when the flow is axial. A device capable of positioning the probe properly must have these requirements: it must be able to maintain the sensor at a fixed point in space while simultaneously allowing for angular variation of the sensor direction with eventual knowledge of the angle relative to some base line. The device consists of a probe holder mounted on a support arm which can be directly attached to the traversing mechanism. The probe holder is manipulated with another extension arm such that the sensor is the center of a circle and the holder is the radius arm which moves in a vertical circular motion. The angular position is indicated on a scale marked directly in degrees by a pointer attached to the extension arm. The device was constructed of aluminum shafts and plexiglas scale and had an overall length of 28 in.

EXPERIMENTAL PROCEDURE

The experimental runs were conducted in distilled water because it would retain its clarity for a longer period and also because it contained less dissolved air. Some low-end data were obtained in air and are shown in the results.

An experimental heat transfer run consisted in placing the sphere supported by the support tube in a rigid assembly, into the center of the tank. Power was then turned on and a steady-state was attained as noted by the e.m.f. measurements of the sphere thermocouples by the potentiometer. Steady-state was assumed when the e.m.f. reading differed by less than 2μV over a 15 min period. The tank bulk temperature was measured with a thermometer and a thermocouple at different positions. They agreed closely with each other. Another run was obtained by increasing the voltage. This procedure continued until the power level for the particular sphere would be excessive under the operating conditions.

The temperature and velocity profile measurements required much initial calibration work. The temperature probe was calibrated, as stated above, and was considered to be accurate to better than 0·1°C. The temperature coefficient of resistance of the hot-film probe was determined by cold resistance measurements in a constant temperature bath. With this information, one could then select a sensor operating temperature from the overheat ratio. Two overheat ratios were chosen: 1·05 and 1·10. There must be a choice between response and bubble formation on the probe, that is to say, that a high overheat ratio gives better response and sensitivity, but it also means a higher temperature which is bounded by the boiling point of the liquid and even more so by the evolution of air bubbles on the sensor. Thus, fresh distilled water was a must. Next, a double calibration was performed by measuring the bridge voltage response at a given temperature for varying velocities of tow, at each overheat ratio. The tank temperatures used with the 1·10 overheat ratio were 22·7, 27·0, 30·0, 35·0, 40·0 and 45·0°C. The velocity ranged from

3×10^{-2} cm/s to 14 cm/s. The tank temperatures used with the 1·05 overheat ratio were 22·7, 27·0 and 30·0°C with the velocities covering the same range as above. Based on an evaluation of this data, it was decided to run at 1·10 overheat for all velocity measurements because of the loss of sensitivity at the 1·05 overheat ratio.

With the hot-film probe fully calibrated, one next proceeds to measure the temperature field at some position normal to the surface of the sphere using the traversing mechanism in conjunction with a cathetometer. Conduction effects along the thermocouple probe were investigated using previously developed analyses [29, 30]. The velocity field at this same position is measured with the hot-film probe, again using the traversing mechanism. We now have bridge voltage and temperature data as a function of distance. Therefore, we can now use the double calibration curves to find the velocities which correspond to the particular distance measurements. Thus, we can fully delineate the velocity profile. The measurements of temperature and velocity fields were confined to the three-inch sphere only and the measurements normal to the sphere surface were taken at the stagnation point, the 45° position, 90° position, and 135° position. A horizontal traverse was taken at the top of the sphere, i.e. cutting across the plume.

Some limited directional measurements were made with the probe located at the 90° position and at various distances from the surface in the horizontal direction. Readings were not taken very close to the surface as was done in the velocity measurements, due to the different probe geometry and angular motion required, together with the very fragile nature of the probe.

RESULTS AND DISCUSSION

Heat transfer experiments

Figure 3 shows the experimental data obtained for laminar free convection heat transfer from isothermal spheres in water. The correlating line was found by the method of least squares to be

$$\overline{Nu} = 2 + C(Gr \,.\, Pr)^{\frac{1}{4}} \tag{14}$$

where $C = 0{\cdot}500 \pm 0{\cdot}009$ and with a mean deviation of less than 11 per cent. The ranges of the variables are: $10 \leqslant \overline{Nu} \leqslant 90$; $3\ (10^5) \leqslant Gr \,.\, Pr \leqslant 8\ (10^8)$.

The air data was not included in the correlation, but is included on the graph for compari-

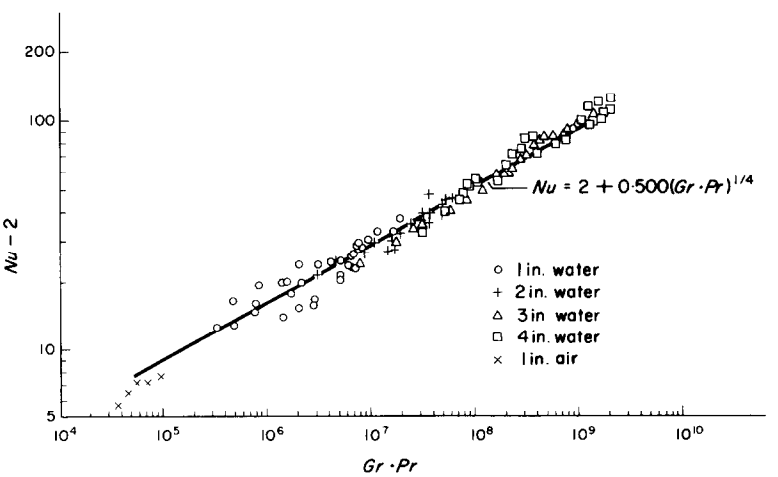

FIG. 3. Experimental data for free convection heat transfer from isothermal spheres in water (based on diameter).

son's sake. Notice that it lies slightly lower than the water data. It is also to be noted that this air data compares very favorably with that of Yuge [1]. Also, only water data up to 8×10^8 is included in this laminar free convection correlation, since turbulence begins shortly thereafter. The value of the constant, namely, 0·500 is lower than the value of 0·59 obtained by Kranse and Schenk [5] in their dissolution studies. Schenkels and Schenk [7] similarly obtain a value of about 0·59, but they note that their data, which have very high Schmidt numbers, seem to be Schmidt number dependent. The work of Jakob and Linke [21] yields a value of 0·555 for the constant, but this constant represents a number of body shapes. Boberg and Starrett [9] obtain the value of 0·51 for this constant which is in close agreement with the value obtained in this work. Vanier [8] obtained 0·52 in his studies of melting ice spheres in water. Merk and Prins [17] theoretical value of 0·558 as with Acrivos' value of 0·583 compare reasonably well when the different forms of the equations are considered. The average deviation over the range of Ra from 10^5 to 10^8 for these theoretical equations when compared to equation (14) is about 6 per cent. This "constant" is a function of Prandtl number and the analyses of Merk and Prins [17] and Acrivos [18] are both based on limiting Prandtl number behavior, i.e. for $Pr \to \infty$. Table 1 shows a comparison of various correlations for free convection heat and mass transfer.

Temperature profile results

The 3 in. sphere was used exclusively for the profile measurement data. Two sets of temperature profile data were obtained. The first set was obtained at a power level of 28 W and the second, at a power level of 112 W. Figures 4 and 5 illustrate the data, with five traverses: stagnation point, 45°, 90°, 135°, and horizontal traverse across the plume at 180°. The temperature layer is thickening slightly on its way up the sphere. The horizontal traverse shows that the temperature distribution is moving into the "plume region" where one would expect a "bell-shaped" distribution, aside from the disturbing aspects of the tube. The stagnation point profile illustrates the finite boundary layer thickness at this position.

The 112 W profiles are shown in Figs. 6 and 7. No stagnation profile was obtained for this run. The horizontal traverse shows the sign of increased activity in the wake region at the higher heat flux. Figure 8 shows the theoretical θ vs. η curve obtained from the solution of equations (8)–(10), compared with the experimental 112 W data. The agreement is seen to be quite good.

Table 1. Comparison of experimental investigations of free convection heat and mass transfer (all based on diameter)

Investigator	Equation	Conditions
Yuge [1]	$\overline{N}u = 2 + 0{\cdot}428\,(Ra)^{\frac{1}{3}}$	Heat transfer-air
Kyte, Madden and Piret [10]	$\overline{N}u = 2 + 0{\cdot}399\,(Ra)^{\frac{1}{3}}$	Heat transfer-air
Ranz and Marshall [11]	$\overline{N}u = 2 + 0{\cdot}6\,Pr^{\frac{1}{12}}Ra^{\frac{1}{4}}$	Evaporation-drops
Kranse and Schenk [5]	$\overline{N}u = 2 + 0{\cdot}59\,(Ra)^{\frac{1}{4}}$	Melting-benzene
Schenkels and Schenk [7]	$\overline{N}u = 2 + 0{\cdot}59\,(Ra)^{\frac{1}{4}}$	Melting-organic spheres
Garner and Keey [3]	$\overline{N}u = 23 + 0{\cdot}585\,(Ra)^{\frac{1}{2}}$	Mass transfer
Garner and Hoffman [12]	$\overline{N}u = 5{\cdot}4 + 0{\cdot}44\,(Ra)^{\frac{1}{2}}$	Mass transfer
Van der Burgh [13]	$\overline{N}u = 0{\cdot}525\,(Ra)^{\frac{1}{4}}$	Melting-benzene
Schenk and Schenkels [6]	$\overline{N}u = 0{\cdot}56\,(Ra)^{\frac{1}{4}}$	Melting-ice spheres
Jakob and Linke [31]	$\overline{N}u = 0{\cdot}555\,(Ra)^{\frac{1}{4}}$	Heat transfer-various body shapes
Vanier [8]	$\overline{N}u = 2 + 0{\cdot}52\,(Ra)^{\frac{1}{4}}$	Melting-ice spheres
Boberg and Starrett [9]	$\overline{N}u = 0{\cdot}51\,(Ra)^{\frac{1}{4}}$	Heat transfer-transient method
Schütz [4]	$\overline{N}u = 2 + 0{\cdot}59\,(Ra)^{\frac{1}{4}}$	Mass transfer-electrochemical

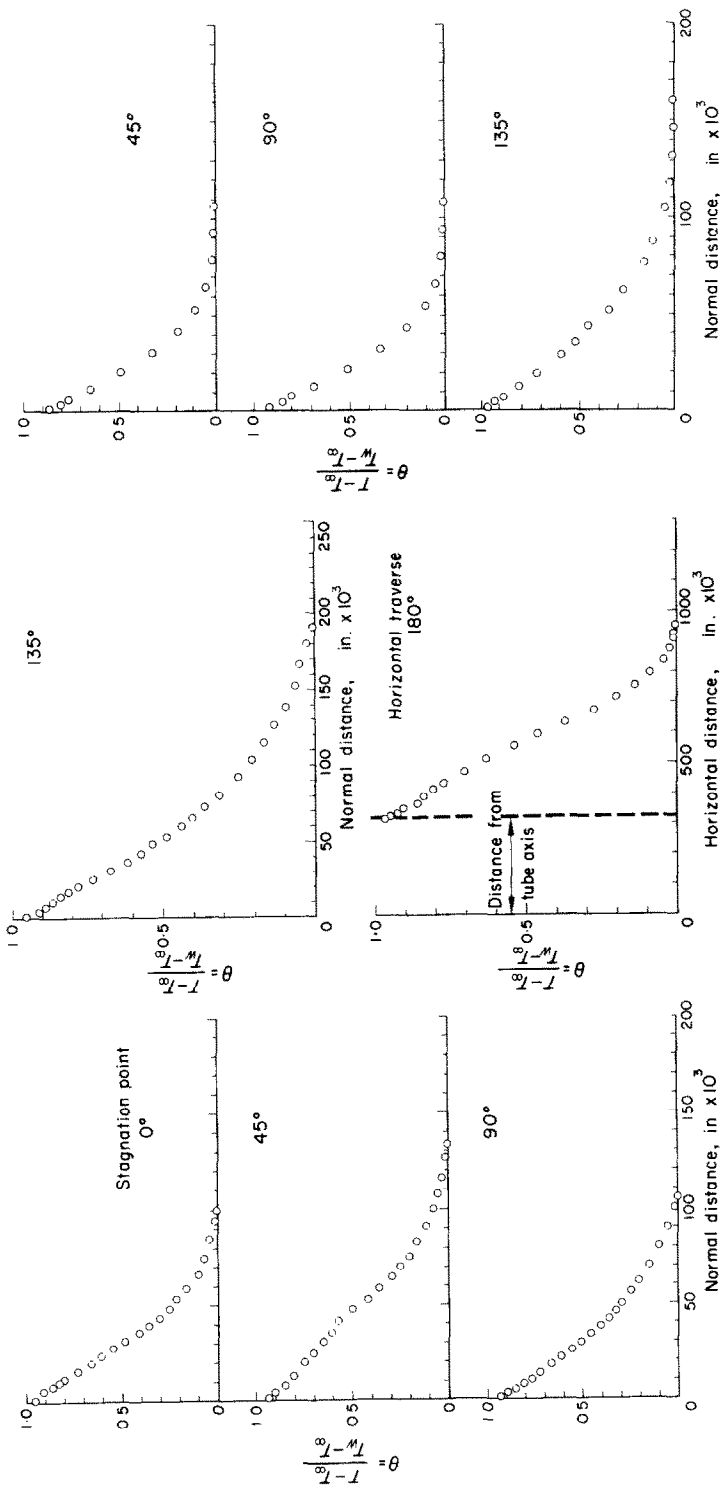

FIG. 4. Temperature profiles: 28 W. 3 in. sphere, $Ra = 4{\cdot}26(10^7)$, water; 0°, 45° and 90° positions.

FIG. 5. Temperature profiles: 28 W. 3 in. sphere, $Ra = 4{\cdot}26\ (10^7)$, water; 135° and 180° (horizontal traverse) positions.

FIG. 6. Temperature profiles: 112 W. 3 in. sphere, $Ra = 1{\cdot}70(10^8)$, water; 45°, 90° and 135° positions.

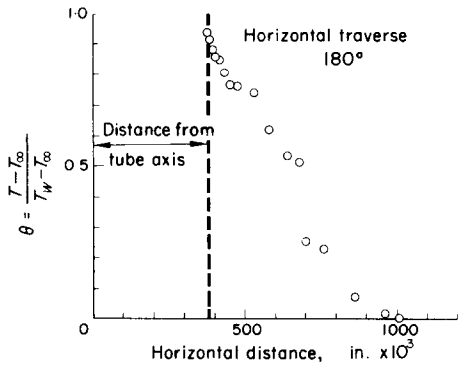

FIG. 7. Temperature profile: 112 W, 3 in. sphere, $Ra = 1{\cdot}70(10^8)$, water; 180° position-horizontal traverse.

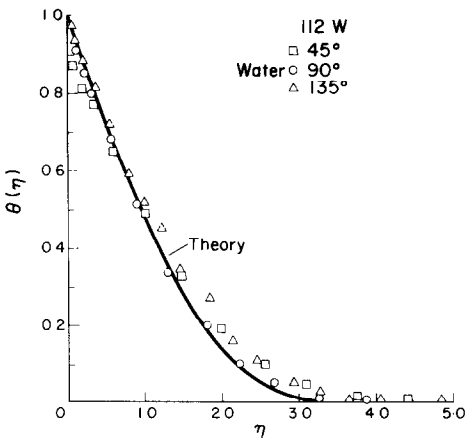

FIG. 8. Dimensionless temperature profile. θ vs. η.

Local heat transfer from a sphere in water

Figure 9 shows the variation in the local heat transfer as a function of the angular distance from the stagnation point compared with the predictions of Acrivos' theory [18]. It can be seen that almost two-thirds of the heat transfer takes place from the bottom half of the sphere.

In order to calculate the local values of heat transfer, it was necessary to least squares fit the profile data at 0°, 45°, 90° and 135° in order to obtain accurate and consistent values of $-\theta'(0)$. The first ten points in the profile were fit to a linear equation according to the following rationale: If the energy equation for heat transfer by free convection is evaluated at the wall, it is immediately true that $\partial^2\theta/\partial y^2|_{y=0}$ equals zero. If the temperature function is expanded in a Taylor series about the point $y = 0$, then it is seen that the use of a linear

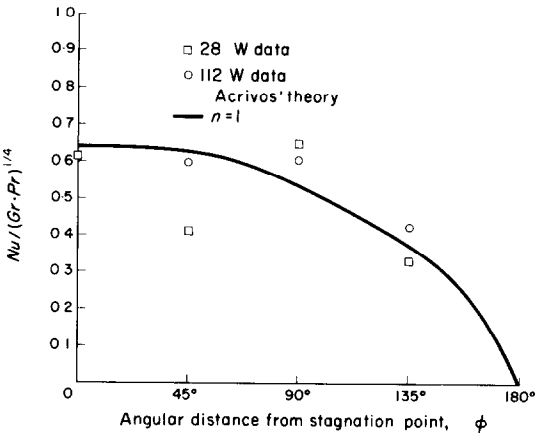

FIG. 9. Variation in local heat transfer rate along sphere in water-based on diameter.

equation is already accurate to terms of $0(y^3)$. An even better fit would be achieved by using a cubic without the quadratic term, but the additional refinement is probably not warranted.

Thermal boundary-layer thickness

Figure 10 shows a plot of a dimensionless boundary-layer thickness vs. dimensionless distance from the stagnation point for the 28 W and 112 W data. The "scaling factor" is the Rayleigh number (average) based on the sphere diameter. The local Rayleigh number was tried as a scaling factor, but the results were not better and it was decided to use the simpler average value.

If one examines the temperature profile curves and the velocity profile curves with respect to boundary-layer thicknesses, the following details are worth noting: (a) There is a finite temperature layer at the stagnation point; (b) The temperature layer appears to be

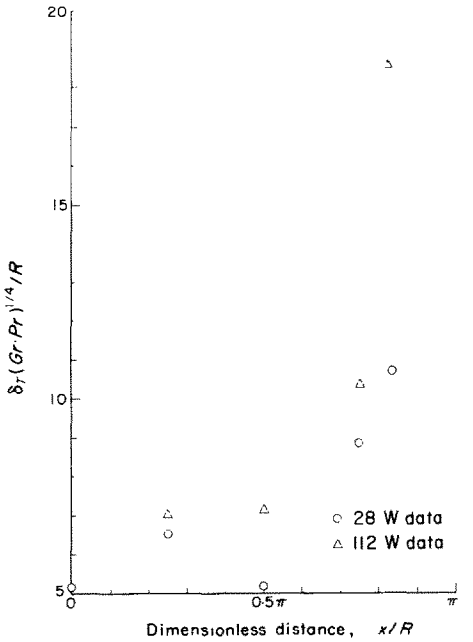

FIG. 10. Dimensionless thermal boundary thickness vs. dimensionless distance from stagnation point for a sphere in water.

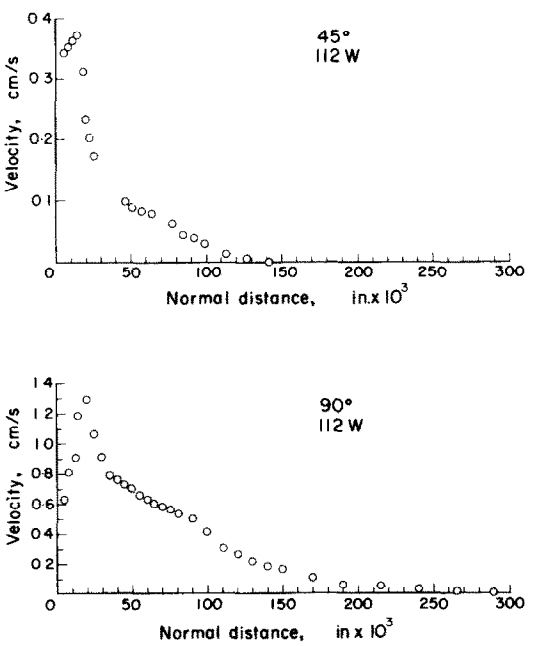

FIG. 11. Velocity profiles: water, 3 in. sphere, 112 W, $Ra = 1{\cdot}70(10^8)$;

slightly thinner than the velocity layer at the 45° position, and grows much more slowly than the velocity layer; (c) After separation has occurred and the flow is moving into the plume, the two layers seem to be approaching equal thicknesses.

Velocity profile results

Figures 11 and 12 show the velocity data obtained with the hot-film anemometry equipment. The resolution is seen to be very good as is the sensitivity. The velocity boundary layer thickens quite rapidly on its way up the sphere. The maximum velocity in the layer was readily discernible and can be seen to be increasing in magnitude in its climb to the plume region.

If use is made of equations (8)–(10), one can estimate the velocities within the thermal boundary layer and compare them against the experimental values. This comparison is shown in

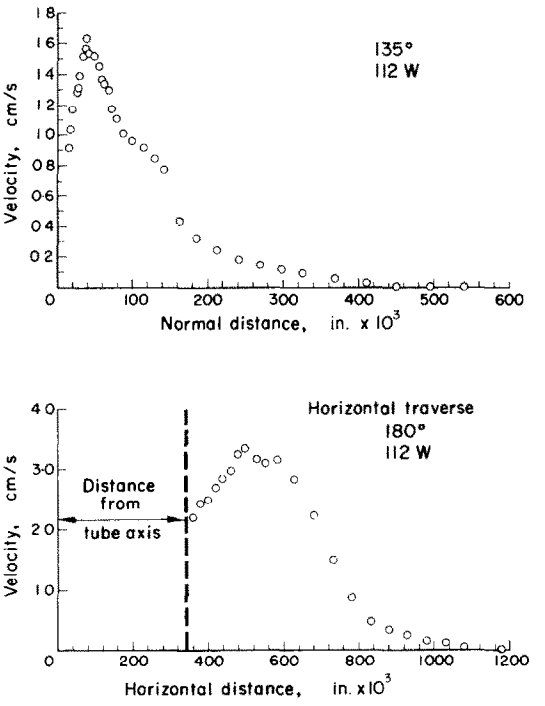

FIG. 12. Velocity profiles: water, 3 in. sphere, 112 W, $Ra = 1{\cdot}70$ (10^8); 135° and 180° (horizontal traverse) positions.

Table 2. Comparison of free convection velocities inside the thermal boundary layer from Acrivos' [18] solution with experimental data

η	$f'(\eta)$	u_{pred} equation (8) (cm/s)	u_{exp} (cm/s)	% diff.
		$x_1 = \pi/4$		
0·261	0·250	0·183	0·342	46·5
0·404	0·392	0·312	0·352	11·4
0·523	0·450	0·358	0·372	3·8
		$x_1 = \pi/2$		
0·203	0·210	0·324	0·69	53·0
0·325	0·310	0·478	0·81	40·9
0·528	0·455	0·702	0·91	22·9
0·609	0·503	0·776	1·19	34·8
0·812	0·600	0·926	1·29	28·2
		$x_1 = 3\pi/4$		
0·434	0·390	0·902	0·92	2·0
0·512	0·440	1·02	1·04	2·1
0·590	0·500	1·15	1·17	1·2
0·668	0·540	1·25	1·29	3·3
0·749	0·575	1·33	1·31	−1·5
0·827	0·610	1·41	1·40	−0·7
0·905	0·636	1·47	1·52	3·3
0·986	0·665	1·54	1·57	2·0
1·064	0·692	1·60	1·64	2·4

Table 2 and indicates that the predictive qualities of the equation for the velocity are fairly good with an average error of 15 per cent for this set of values.

Merk and Prins' [17] work will be used to compare the values of maximum velocity measured in the velocity traverses. Their results are in the form of a plot of $u_{max}D/\nu Gr^{\frac{1}{2}}$ vs. the angular distance from the stagnation point, with Prandtl number as parameter. Thus, it is quite easy to compare these values to the maximums obtained experimentally. Table 3 illustrates the comparison. The agreement is good, especially for velocity profile data.

Table 3. Comparison of Merk and Prins' [17] prediction of maximum velocity in free convection with experimental data, for a sphere

ϕ	u_{max} Merk and Prins' [17] prediction cm/s	u_{max} Experimental this work cm/s	% Diff.
45°	0·43	0·375	−14·6
90°	1·08	1·29	+16·3
135°	1·49	1·64	+9·1

CONCLUSIONS

The laminar free convection heat transfer from isothermal spheres to water may be characterized by

$$\overline{Nu} = 2 + C(Gr \,.\, Pr)^{\frac{1}{4}}$$

where $C = 0{\cdot}500 \pm 0{\cdot}009$ and with a mean deviation of less than 11 per cent for $3\ (10^5) \leqslant Gr \,.\, Pr \leqslant 8\ (10^8)$.

The temperature and velocity fields have been measured around a sphere and it has been demonstrated that hot-film anemometry can be effectively utilized in non-isothermal liquid, free convection systems.

ACKNOWLEDGEMENTS

The authors wish to thank the National Science Foundation for its financial support, in part, through Grant No. GK-408. One of the authors (W.S.A.) also wishes to acknowledge the financial support in the form of an NDEA Fellowship during the period 1965–1968 at Syracuse University.

REFERENCES

1. T. YUGE, Experiments on heat transfer from spheres

including natural and forced convection. *J. Heat Transfer* **820**, 214–220 (1960).
2. W. ELENBAAS, The dissipation of heat by free convection – horizontal and vertical cylinders; spheres, *Physica* **IX** (7), 665–672 (1942).
3. F. H. GARNER and R. B. KEEY, Mass transfer from single solid spheres – I, *Chem. Engng Sci.* **9**, 119–129 (1958).
4. G. SCHÜTZ, Natural convection mass transfer measurements on spheres and horizontal cylinders by an electrochemical method, *Int. J. Heat Mass Transfer* **6**, 873–879 (1963).
5. A. A. KRANSE and J. SCHENK, Thermal free convection from a solid sphere, *Appl. Sci. Res.* **A15**, 397–403 (1965).
6. J. SCHENK and F. A. M. SCHENKELS, Thermal free convection from an ice sphere in water, *Appl. Sci. Res.* **19**, 465–476 (1868).
7. F. A. M. SCHENKELS and J. SCHENK, Dissolution of solid spheres by isothermal free convection, *Chem. Engng Sci.* **24**, 585–593 (1969).
8. C. R. VANIER, M.S. Thesis, Dept. of Chemical Engineering, Syracuse University, Syracuse, N.Y. (1967).
9. J. E. BOBERG and P. S. STARRETT, Determination of the free convection heat transfer properties of fluids, *Ind. Engng Chem.* **50**, 807–810 (1958).
10. J. R. KYTE, A. J. MADDEN and E. L. PIRET, Natural convection heat transfer at reduced pressure, *Chem. Engng Prog.* **49**, 653–662 (1953).
11. W. E. RANZ and W. R. MARSHALL, JR., Evaporation from drops, *Chem. Engng Prog.* **48**, 173–180 (1952).
12. F. H. GARNER and J. M. HOFFMAN, Mass transfer from single solid spheres by free convection, *A.I.Ch.E.Jl* **7**, 148–152 (1961).
13. J. VAN DER BURGH, Thermal convection at a melting benzene surface, *Appl. Sci. Res.* **A9**, 293–296 (1960).
14. R. S. SCHECHTER and H. J. ISBIN, Natural convection heat transfer in regions of maximum fluid density, *A.I.Ch.E.Jl* **4**, 81–89 (1958).
15. R. P. DRING and B. GEBHART, Hot-wire anemometer calibration at very low velocity, *J. Heat Transfer* **91C**, 241–244 (1969).
16. G. C. VLIET and C. K. LIU, An experimental study of turbulent natural convection boundary layers, *J. Heat Transfer* **91C**, 517–531 (1969).
17. H. J. MERK and J. A. PRINS, Thermal convection in Laminar boundary layers, I, II, III, *Appl. Sci. Res.* **A4**, 1, 3, 11–24, 195–206, 207–222 (1953, 1954).
18. A. ACRIVOS, A theoretical analysis of laminar natural convection heat transfer to non-Newtonian fluids, *A.I.Ch.E.Jl* **6**, 584–590 (1960).
19. D. A. SAVILLE, Ph.D. Dissertation, Univ. of Michigan, Ann Abor (1965).
20. D. A. SAVILLE and S. W. CHURCHILL, Laminar free convection in boundary layers near horizontal cylinders and vertical axisymmetric bodies, *J. Fluid Mech.* **29**, 391–399 (1967).
21. D. A. SAVILLE and S. W. CHURCHILL, Simultaneous heat and mass transport in free convection boundary layers, *A.I.Ch.E.Jl* **16**, 268–272 (1970).
22. T. CHIANG, A. OSSIN and C. L. TIEN, Laminar free convection from a sphere, *J. Heat Transfer* **86C**, 537–541 (1964).
23. L. V. KING, On the convection of heat from small cylinders in a stream of fluid: determination of the convection constants of small platinum wires with applications to hot-wire anemometry, *Phil. Trans. R. Soc., Lond.* **214A**, 373–433 (1914).
24. N. A. V. PIERCY, E. G. RICHARDSON and H. F. WINNEY, On the convection of heat from a wire moving through air close to a cooling surface, *Proc. Phys. Soc., Lond.* **B69**, 731–742 (1956).
25. J. A. R. WILLS, The correction of hot-wire readings for proximity to a solid boundary, *J. Fluid Mech.* **12**, 388–396 (1962).
26. E. G. RICHARDSON, The correction of hot-wire readings in a boundary layer for proximity to the solid boundary, *J. Aero. Sci.* **23**, 970–971 (1956).
27. W. S. AMATO, Ph.D. Dissertation, Syracuse University, Syracuse, New York (1970).
28. W. F. ROESER and H. T. WENSEL, *Temperature: Its Measurement and Control in Science and Industry*, pp. 284–313, American Institute of Physics, Reinhold Publishing Corp., New York (1941).
29. M. JAKOB, The influence of the free end of a rod on heat transfer, *Phil. Mag.* **28**, 571–578 (1939).
30. E. F. C. SOMERSCALES, Ph.D. Dissertation, Cornell University, Ithaca, New York (1965).
31. M. JAKOB and W. LINKE, Der Wärmeübergang von einer waagerechten Platte an siedendes Wasser, *Forsch. Geb. Ing.* **4**, 75–81 (1933).

TRANSFERT THERMIQUE PAR CONVECTION NATURELLE À PARTIR DE SPHÈRES ISOTHERMES DANS L'EAU

Résumé—On présente une recherche expérimentale du transfert thermique par convection naturelle entre des sphères chauffées et de l'eau. Les résultats expérimentaux s'étendent sur un large domaine du nombre de Rayleigh couvrant ainsi les régimes laminaires, de transition et le régime turbulent naissant. On a mesuré les champs de température et de vitesse autour d'une sphère isotherme chauffée, avec les profils de vitesse déterminés par la technique de l'anémomètre à film chaud. Chaque fois que possible, la comparaison des résultats expérimentaux avec la prédiction théorique montrent un bon accord.

FREIE KONVEKTION AN ISOTHERMEN KUGELN IN WASSER

Zusammenfassung—Es wird über eine experimentelle Untersuchung des Wärmeübergangs durch freie Konvektion von beheizten Kugeln an Wasser berichtet. Die experimentellen Ergebnisse erstrecken sich über einen weiten Bereich der Rayleigh-Zahl und erfassen so das laminare, das Übergangs- und den Beginn des turbulenten Gebiets. Das Temperatur- und Geschwindigkeitsfeld um eine beheizte, isotherme Kugel wurde gemessen, wobei zur Bestimmung der Geschwindigkeitsprofile Heissfilmanemometer benutzt wurden. Soweit ein Vergleich der experimentellen Daten mit theoretischen Voraussagen möglich war, zeigte sich gute Übereinstimmung.

СВОБОДНАЯ КОНВЕКЦИЯ ОТ ИЗОТЕРМИЧЕСКИХ НАГРЕТЫХ СФЕР В ВОДЕ

Аннотация—Представлено экспериментальное исследование теплообмена при свободной конвекции от нагретых сфер к воде. Экспериментальные данные представлены для широкого диапазона значений числа Релея, включая ламинарный, переходный и начало турбулентного режимов. Были измерены поля температуры и скорости вокруг изотермически нагретой сферы, профили скорости определялись анемометром с нагретой пленкой. Сравнение экспериментальных результатов с теоретическими дают хорошее согласие.